PHYSICAL REVIEW D **95,** 054027 (2017)

$P_c(4380)$ in a constituent quark model

Woosung Park,[1,*] Aaron Park,[1,†] Sungtae Cho,[2,‡] and Su Houng Lee[1,§]

[1]*Department of Physics and Institute of Physics and Applied Physics, Yonsei University, Seoul 03722, Korea*

[2]*Division of Science Education, Kangwon National University, Chuncheon 24341, Korea*

(Received 3 February 2017; published 31 March 2017)

The constituent quark model with color-spin hyperfine potential is used to investigate the property of a compact pentaquark configuration with $J^p = 3/2^-$ and isospin $= 1/2$, which is the most likely quantum number of one of the recently observed exotic baryon states at LHCb. Starting from the characterization of the isospin, color, and spin states for the pentaquark configuration, we construct the total wave function composed of the spatial wave function, which we take to be symmetric and in S wave, and the four orthogonal isospin $\otimes$ color $\otimes$ spin states that satisfy the Pauli principle. We then use the variational method to find a compact stable configuration. While there are compact configurations where the hyperfine potential is more attractive than the sum of p and J/ψ hyperfine potentials, we find that the ground state is the isolated p and J/ψ state. Furthermore, the mass of the excited state lies far above the observed pentaquark state leading us to conclude that the observed states cannot be a compact configuration with $J^p = 3/2^-$, generated by the conventional two-body quark interactions.

DOI: 10.1103/PhysRevD.95.054027

I. INTRODUCTION

After the introduction of the quark model for the baryon and meson [1] and the color quantum number for quarks [2], model calculations for hadrons naturally led to the possible existence of mutiquark hadrons beyond the ordinary hadrons [3,4]. Indeed, recent experimental findings point to the possible existence of such configurations; these are the XYZ states with the $X(3872)$ being the first of these states observed by the Belle collaboration [5]. The XYZ states could be either compact tetraquark states composed of two quarks and two antiquarks or molecular states with their masses close to the relevant two meson thresholds.

Molecular configurations involving heavy mesons were first discussed in Ref. [6] where deuteronlike meson-meson bound states were found to exist when a long range pion exchange potential was included with additional short range attraction depending on the mass of the meson. The possible bound states included a $D\bar{D}^*$ state in the isopin 0 and $J^{PC} = 1^{++}$ channel, which is the quantum number of the $X(3872)$. Since the experimental observation of $X(3872)$, attempts to explain the state in terms of molecular configuration with important contribution coming from the pion exchange potentials have continued to this date [7–11].

Numerous efforts have been made to explain the mass of the charmoniumlike state using various other approaches. In a nonrelativistic quark model that includes a confining interaction and a short range spin-dependent interaction through the one gluon exchange as well as an effective pion-induced interaction, it was argued that the $X(3872)$ can be a $D\bar{D}^*$ hadronic resonance with important admixtures of $\rho J/\psi$ and $\omega J/\psi$ states [12]. In Ref. [13], the $X(3872)$ was considered as a weakly bound molecular state found in the combination of $\{D, D^*\}$ with $\{\bar{D}, \bar{D}^*\}$ states based on a quark-based nonrelativistic four-body Hamiltonian with a pairwise interaction.

There are also models that find $X(3872)$ to be a tetraquark system. These include methods based on a diquark-antidiquark model [14,15], the QCD sum rule [16], and a simple quark model with chromomagnetic interactions [17–19]. In a lattice QCD calculation [20], it was shown that a candidate for $X(3872)$ with $I = 0$ could only be found if both the $\bar{c}c$ and $\bar{D}\bar{D}^*$ interpolators are included, while no signal was found if the diquark-antidiquark and $\bar{D}\bar{D}^*$ are used without a $\bar{c}c$ component.

Recently, the observation of hidden-charm pentaquark states by the LHCb collaboration [21] has triggered another wave of works among many researchers. The $J/\psi p$ invariant mass spectrum of $\Lambda_b \to J/\psi K^- p$ revealed hidden-charm pentaquark states, for which the preferred quantum numbers are $J^p = 3/2^-$ for $P_c(4380)$ and $J^p = 5/2^+$ for $P_c(4450)$. In fact, even before the discovery was made, possible hidden-charm molecular baryons composed of anticharmed meson and charmed baryon, such as the of $\Sigma_c\bar{D}^*$ states with $I(J^p) = \frac{1}{2}(\frac{1}{2}^-)$, $\frac{1}{2}(\frac{3}{2}^-)$, $\frac{3}{2}(\frac{1}{2}^-)$, $\frac{3}{2}(\frac{3}{2}^-)$, and $\Sigma_c\bar{D}$ states with $\frac{3}{2}(\frac{1}{2}^-)$, were proposed to exist within the one-boson-exchange model [22]. The two hidden-charm pentaquark states were also found to be loosely bound $\Sigma_c\bar{D}^*$ and $\Sigma_c^*\bar{D}^*$ molecular states, respectively, within a

*diracdelta@hanmail.net
†aaron.park@yonsei.ac.kr
‡sungtae.cho@kangwon.ac.kr
§suhoung@yonsei.ac.kr

boson-exchange interaction model [23]. Furthermore, in a meson exchange model [25], $P_c(4380)$ with $J^p = 3/2^-$ was produced from $\Sigma_c^* \bar{D}$, while $P_c(4450)$ with $J^p = 5/2^+$ was produced from $\Sigma_c \bar{D}^*$. More recently, the pentaquarks were identified with structures around the $\Sigma_c^{(*)} \bar{D}^{(*)}$ threshold in a quark cluster model [24].

While molecular pictures for the two pentaquark states are quite likely, one can not rule out the possibility that these states are compact multiquark configurations based on a strong diquark-antidiquark pair [26] or quark interactions in general [27]. To distinguish these two configurations, it is important to fully explore these two possible scenarios. In this work, we explore the possibility that one of the pentaquarks is a compact multiquark configuration within a constituent quark model based on the color and spin hyperfine potential [28], which is known to reproduce the masses of the ordinary meson and baryon states. In particular, in order to asses the possibility that the $P_c(4380)$ is a compact multiquark state, we classify the isospin, color, and spin states for the pentaquark system containing a heavy quark and an antiquark with $J^p = 3/2^-$ and isospin $= 1/2$ from the view point of the permutation group, which is used in characterizing a certain symmetry so that the isospin, color, and spin states can be represented in terms of the Young-Yamanouchi bases. We then systematically construct the isospin $\otimes$ color $\otimes$ spin states satisfying the Pauli principle from the coupling scheme appearing in the combination of any two states. We then use the variational method to calculate the ground state mass of the pentaquark with $J^p = 3/2^-$ and isospin $= 1/2$.

This paper is organized as follows. In Sec. II, we first introduce the Hamiltonian describing the constituent quark model, and determine the fitting parameters of the model so as to reproduce the mass of the baryons and mesons associated with the thresholds. Then, by using the variational method, we construct the spatial wave function suitable for a baryon and a meson. In Sec. III, we represent the isospin, color, and spin states and then construct the isospin $\otimes$ color $\otimes$ spin states with respect to $I = 3/2$ and $I = 1/2$ in two independent bases, which can be transformed into each other through an orthonormal matrix. We analyze the numerical results obtained from the variational method in Sec. IV. We finally give a summary of the paper in Sec. V.

II. HAMILTONIAN

To investigate the stability of the pentaquark in the nonrelativistic framework, the Hamiltonian is chosen to take the confinement and hyperfine potential for the color and spin interaction;

$$H = \sum_{i=1}^{5} \left(m_i + \frac{\mathbf{p}_i^2}{2m_i} \right) - \frac{3}{16} \sum_{i<j}^{4} \lambda_i^c \lambda_j^c (V_{ij}^C + V_{ij}^{SS}), \quad (1)$$

where m_i's are the quark masses, $\lambda_i^c/2$ the color operator of the ith quark for the color SU(3), and V_{ij}^C and V_{ij}^{SS} the confinement and hyperfine potential, respectively. The confinement potential is usually composed of the linearizing term as suggested by the lattice gauge theory, and the Coulomb-type potential as derived from the perturbative QCD,

$$V_{ij}^C = -\frac{\kappa}{r_{ij}} + \frac{(r_{ij})^{1/2}}{a_0} - D. \quad (2)$$

The hyperfine potential is given to take the following form, including the spin interaction:

$$V_{ij}^{SS} = \frac{1}{m_i m_j c^4} \frac{\hbar^2 c^2 \kappa'}{(r_{0ij})} \frac{e^{-(r_{ij})^2/(r_{0ij})^2}}{r_{ij}} \sigma_i \cdot \sigma_j. \quad (3)$$

Here, r_{ij} is the distance between quarks, $|\mathbf{r}_i - \mathbf{r}_j|$, and both r_{0ij} and κ' are chosen to depend on the masses of quarks, given by

$$r_{0ij} = 1/\left(\alpha + \beta \frac{m_i m_j}{m_i + m_j} \right),$$
$$\kappa' = \kappa_0 \left(1 + \gamma \frac{m_i m_j}{m_i + m_j} \right). \quad (4)$$

The hyperfine potential in Eq. (3), which becomes $1/(m_i m_j)\ \delta(r)$ in the heavy quark mass limit $m_i \to \infty$, is chosen to fit the meson and baryon mass splitting with both light and heavy quarks. The parameters in the Hamiltonian are fitted to the baryon and meson masses by using the variational method [29]. The fitting parameters are given in Table I, and the calculated masses in Table II.

Since we deal with the pentaquark composed of $q(1)q(2)q(3)c(4)\bar{c}(5)$ with $I = 1/2$, where the number indicates the position of the constituent quark, the symmetry of the three light quarks should be taken into account to satisfy the Pauli principle because the total wave function must be antisymmetric among the three light quarks. As we are interested in the ground state, a natural choice would be to take the spatial function to be symmetric, which requires

TABLE I. Parameters of the Hamiltonian fitted to the baryon and meson masses occurring in the decay channels of the $q^3 c\bar{c}$.

γ	κ	a_0	D	κ_0	α	β	m_u	m_c
1.667 (GeV)$^{-1}$	0.107	1.042 (GeV)$^{-2}$	0.955 GeV	0.168 GeV	1.224 GeV	1.467	0.302 GeV	1.889 GeV

TABLE II. Masses of baryons and mesons obtained from the variational method. The third row shows the variational parameter in fm^{-2}. The fourth row shows the experimental data in GeV.

(I,S)	$(\frac{1}{2},\frac{1}{2})$ P	$(\frac{3}{2},\frac{3}{2})$ Δ	$(0,\frac{1}{2})$ Λ_c	$(1,\frac{1}{2})$ Σ_c	$(1,\frac{3}{2})$ Σ_c^*	(0,0) η_c	(0,1) J/ψ	$(\frac{1}{2},0)$ D	$(\frac{1}{2},1)$ D^*
Mass	0.972	1.266	2.286	2.459	2.536	2.984	3.115	1.872	2.012
Variational parameters	a=3.4, b=1.4	a=2.1, b=1.2	a=2.7, b=3.4	a=1.9, b=3.5	a=1.8, b=3.1	a=15.1	a=11	a=4.4	a=3.4
Exp	0.938	1.232	2.286	2.453	2.518	2.983	3.96	1.869	2.01

the remaining part of the total wave function to be antisymmetric among the three light quarks. We denote the symmetry (antisymmetry) property by [123] ({123}). In the center of mass frame, the pentaquark system is reduced to a four-body problem, represented by the four Jacobian coordinates suitable for describing the decay into a baryon and a meson.

We take the spatial function to be a Gaussian that was extensively used with the variational method to handle calculations in the many-body problem. The four Jacobian coordinates suitable for describing the decay into a baryon and a meson are given by

$$\begin{aligned}
\boldsymbol{x}_1^1 &= \frac{1}{\sqrt{2}}(\mathbf{r}_1-\mathbf{r}_2), \qquad \boldsymbol{x}_2^1 = \sqrt{\frac{2}{3}}\left(\mathbf{r}_3-\frac{1}{2}\mathbf{r}_1-\frac{1}{2}\mathbf{r}_2\right),\\
\boldsymbol{x}_3^1 &= \frac{1}{\sqrt{2}}(\mathbf{r}_4-\mathbf{r}_5),\\
\boldsymbol{x}_4^1 &= \sqrt{\frac{6}{5}}\left(\frac{1}{3}(\mathbf{r}_1+\mathbf{r}_2+\mathbf{r}_3)-\frac{1}{2}(\mathbf{r}_4+\mathbf{r}_5)\right),
\end{aligned}\tag{5}$$

where the first and second terms represent a baryon configuration, the third a meson configuration, and the last the relative position vector between the center of mass of a baryon and a meson. The boldface letters stand for the vectors.

We then construct a spatial wave function given by

$$R^{s_1} = \exp[-a_1(\boldsymbol{x}_1^1)^2 - a_2(\boldsymbol{x}_2^1)^2 - a_3(\boldsymbol{x}_3^1)^2 - a_4(\boldsymbol{x}_4^1)^2], \tag{6}$$

where a_1, a_2, a_3, and a_4 are variational parameters. Since the spatial wave function in Eq. (6) is symmetric only between particles 1 and 2, we need two additional spatial wave functions so as to satisfy [123] symmetry; one is symmetric between particles 1 and 3, and the other is symmetric between particles 2 and 3. The two sets of four Jacobian coordinates are given by

$$\begin{aligned}
\boldsymbol{x}_1^2 &= \frac{1}{\sqrt{2}}(\mathbf{r}_1-\mathbf{r}_3), \qquad \boldsymbol{x}_2^2 = \sqrt{\frac{2}{3}}\left(\mathbf{r}_2-\frac{1}{2}\mathbf{r}_1-\frac{1}{2}\mathbf{r}_3\right),\\
\boldsymbol{x}_3^2 &= \frac{1}{\sqrt{2}}(\mathbf{r}_4-\mathbf{r}_5),\\
\boldsymbol{x}_4^2 &= \sqrt{\frac{6}{5}}\left(\frac{1}{3}(\mathbf{r}_1+\mathbf{r}_2+\mathbf{r}_3)-\frac{1}{2}(\mathbf{r}_4+\mathbf{r}_5)\right),
\end{aligned}\tag{7}$$

$$\begin{aligned}
\boldsymbol{x}_1^3 &= \frac{1}{\sqrt{2}}(\mathbf{r}_2-\mathbf{r}_3), \qquad \boldsymbol{x}_2^3 = \sqrt{\frac{2}{3}}\left(\mathbf{r}_1-\frac{1}{2}\mathbf{r}_2-\frac{1}{2}\mathbf{r}_3\right),\\
\boldsymbol{x}_3^3 &= \frac{1}{\sqrt{2}}(\mathbf{r}_4-\mathbf{r}_5),\\
\boldsymbol{x}_4^3 &= \sqrt{\frac{6}{5}}\left(\frac{1}{3}(\mathbf{r}_1+\mathbf{r}_2+\mathbf{r}_3)-\frac{1}{2}(\mathbf{r}_4+\mathbf{r}_5)\right).
\end{aligned}\tag{8}$$

By using the two sets of four Jacobian coordinates, we construct the spatial wave function with either [13] symmetry or [23] symmetry, respectively. Combining these spatial functions with a certain symmetry into a linear form, we obtain the spatial function with four variational parameters a_1, a_2, a_3, and a_4, which is fully symmetric among particles 1–3 as follows:

$$\begin{aligned}
R = {}& \exp[-a_1(\boldsymbol{x}_1^1)^2 - a_2(\boldsymbol{x}_2^1)^2 - a_3(\boldsymbol{x}_3^1)^2 - a_4(\boldsymbol{x}_4^1)^2]\\
&+ \exp[-a_1(\boldsymbol{x}_1^2)^2 - a_2(\boldsymbol{x}_2^2)^2 - a_3(\boldsymbol{x}_3^2)^2 - a_4(\boldsymbol{x}_4^2)^2]\\
&+ \exp[-a_1(\boldsymbol{x}_1^3)^2 - a_2(\boldsymbol{x}_2^3)^2 - a_3(\boldsymbol{x}_3^3)^2 - a_4(\boldsymbol{x}_4^3)^2].
\end{aligned}\tag{9}$$

The spatial wave function of the pentaquark in Eq. (9) is in a state with total angular moment $L=0$, where both the baryon and meson configurations as well as their relative motion is in the S-wave state. The kinetic energy part coming from Eq. (9) is given as

$$K.E. = \frac{\mathbf{p}_1^2+\mathbf{p}_2^2}{2m_1} + \frac{\mathbf{p}_3^2}{2m_2} + \frac{\mathbf{p}_4^2}{2\mu}. \tag{10}$$

Here $\mathbf{p}_1^2+\mathbf{p}_2^2=3\hbar^2 f(a_1,a_2)$, $\mathbf{p}_3^2=3\hbar^2 a_3$, and $\mathbf{p}_4^2=3\hbar^2 a_4$, where m_1, m_2 are the light and heavy quark masses respectively, and $\mu = 5m_1m_2/(3m_1+2m_2)$. We present $f(a_1,a_2)$ appearing in the kinetic terms of the baryon,

$$\begin{aligned}
f(a_1,a_2) = {}&(a_1+a_2)\\
&\times\left\{\frac{1}{(a_1a_2)^{(3/2)}} + \frac{2048a_1a_2}{(3a_1{}^2+10a_1a_2+3a_2{}^2)^{(3/2)}}\right\}\Big/\\
&\times\left\{\frac{2}{(a_1a_2)^{(3/2)}} + \frac{256a_1a_2}{(3a_1{}^2+10a_1a_2+3a_2{}^2)^{(3/2)}}\right\}.
\end{aligned}\tag{11}$$

Hence, for the compact multiquark state to be stable compared to the separated baryon and meson state, the extra attraction coming from bringing the baryon and meson should be large enough to overcome the extra kinetic energy given by the last term in Eq. (10).

III. ISOSPIN ⊗ COLOR ⊗ SPIN STATE OF THE PENTAQUARK

In this section, we construct the isospin ⊗ color ⊗ spin state appropriate for the $q(1)q(2)q(3)Q(4)\bar{Q}(5)$ system with $I = 1/2$ and spin $= 3/2$, where the number in the bracket indicates the position of the constituent quark. The component of three identical light quarks of the pentaquark restricts the total wave function to be antisymmetric with respect to the exchange of any pair among the three light quarks due to the Pauli principle. When the spatial function of the pentaquark is chosen to be fully symmetric for the three light quarks, the remaining part of the total wave function should be fully antisymmetric. Therefore, as we are interested in the ground state, the symmetry property of the isospin ⊗ color ⊗ spin state should be taken to be antisymmetric for particles 1–3. We use $\{123\}$ notation for the antisymmetry property. The Young tableau, which represents the irreducible bases of the permutation group, enables us to easily identify the multiquark configuration with a certain symmetry property. In this paper, we use the Young tableau and the Young-Yamanouchi basis, which corresponds to the Young tableau in describing the states necessary for the pentaquark. In the following subsections, we first start by separately discussing the isospin, color, and spin states consisting of five quarks, and then discuss the total wave function.

A. Isospin states

In the SU(2) flavor symmetry, it is easy to find that the possible isospin (I) states for the three light quarks are $1/2$ and $3/2$. The Young-Yamanouchi basis corresponding to the $I = 1/2$ state is as follows:

$$
\begin{aligned}
|I_1^{1/2}\rangle &= \begin{array}{|c|c|}\hline 1 & 2 \\ \hline 3 & \multicolumn{1}{c}{} \\ \cline{1-1}\end{array} = \frac{1}{\sqrt{6}}(2uud - udu - duu), \\
|I_2^{1/2}\rangle &= \begin{array}{|c|c|}\hline 1 & 3 \\ \hline 2 & \multicolumn{1}{c}{} \\ \cline{1-1}\end{array} = \frac{1}{\sqrt{2}}(udu - duu).
\end{aligned} \tag{12}
$$

B. Color states

For the possible color states, we only consider the color singlets that are assumed to be observables in the hadron state. There are several ways of obtaining the color singlets for the pentaquark, coming from the direct product, given by

$$[3]_C \otimes [3]_C \otimes [3]_C \otimes [3]_C \otimes [\bar{3}]_C.$$

We introduce the two methods that are equivalent to each other, but different in the way of combining the irreducible representation of SU(3). First, since the antiquark corresponds to the antitriplet, we can construct the triplet in the direct product, $[3]_C \otimes [3]_C \otimes [3]_C \otimes [3]_C$, which corresponds to the Young tableau [211],

$$
\begin{aligned}
&\begin{array}{|c|c|}\hline 1 & 2 \\ \hline 3 & \multicolumn{1}{c}{} \\ \cline{1-1} 4 & \multicolumn{1}{c}{} \\ \cline{1-1}\end{array} = \{(12)_6(34)_{\bar{3}}\}_3, \quad
\begin{array}{|c|c|}\hline 1 & 3 \\ \hline 2 & \multicolumn{1}{c}{} \\ \cline{1-1} 4 & \multicolumn{1}{c}{} \\ \cline{1-1}\end{array} = \{(12)_{\bar{3}}34\}_3, \\
&\begin{array}{|c|c|}\hline 1 & 4 \\ \hline 2 & \multicolumn{1}{c}{} \\ \cline{1-1} 3 & \multicolumn{1}{c}{} \\ \cline{1-1}\end{array} = \{(123)_1 4\}_3.
\end{aligned} \tag{13}
$$

Here, the subscript indicates the irreducible representation of SU(3). Then, we can obtain the three color singlets, combining the triplet in Eq. (13) with the antitriplet of the antiquark. We denote the color singlets by

$$
\begin{aligned}
&|C_1\rangle = \begin{array}{|c|c|}\hline 1 & 2 \\ \hline 3 & \multicolumn{1}{c}{} \\ \cline{1-1} 4 & \multicolumn{1}{c}{} \\ \cline{1-1}\end{array}_{\,3} \otimes (5)_{\bar{3}}, \quad
|C_2\rangle = \begin{array}{|c|c|}\hline 1 & 3 \\ \hline 2 & \multicolumn{1}{c}{} \\ \cline{1-1} 4 & \multicolumn{1}{c}{} \\ \cline{1-1}\end{array}_{\,3} \otimes (5)_{\bar{3}}, \\
&|C_3\rangle = \begin{array}{|c|c|}\hline 1 & 4 \\ \hline 2 & \multicolumn{1}{c}{} \\ \cline{1-1} 3 & \multicolumn{1}{c}{} \\ \cline{1-1}\end{array}_{\,3} \otimes (5)_{\bar{3}}.
\end{aligned} \tag{14}
$$

Secondly, we can decompose the direct product, $[3]_C \otimes [3]_C \otimes [3]_C$ and $\otimes\, [3]_C \otimes [\bar{3}]_C$, into the direct sum of the irreducible representations, respectively, as follows:

$$
[3]_C \otimes [3]_C \otimes [3]_C = \begin{array}{|c|c|}\hline 1 & 2 \\ \hline 3 & \multicolumn{1}{c}{} \\ \cline{1-1}\end{array}_{\,8} \oplus \begin{array}{|c|c|}\hline 1 & 3 \\ \hline 2 & \multicolumn{1}{c}{} \\ \cline{1-1}\end{array}_{\,8} \oplus \begin{array}{|c|}\hline 1 \\ \hline 2 \\ \hline 3 \\ \hline\end{array}_{\,1}, \tag{15}
$$

$$[3]_C \otimes [\bar{3}]_C = [8]_C \oplus [1]_C. \tag{16}$$

Then, the coupling of either the octet with the octet or the singlet with the singlet in Eqs. (15) and (16) gives the three color singlets of the pentaquark, denoted by

$$
\begin{aligned}
&|C_1\rangle = \begin{array}{|c|c|}\hline 1 & 2 \\ \hline 3 & \multicolumn{1}{c}{} \\ \cline{1-1}\end{array}_{\,8} \otimes (45)_8, \quad
|C_2\rangle = \begin{array}{|c|c|}\hline 1 & 3 \\ \hline 2 & \multicolumn{1}{c}{} \\ \cline{1-1}\end{array}_{\,8} \otimes (45)_8, \\
&|C_3\rangle = \begin{array}{|c|}\hline 1 \\ \hline 2 \\ \hline 3 \\ \hline\end{array}_{\,1} \otimes (45)_1.
\end{aligned} \tag{17}
$$

It should be noted that the color singlets represented in terms of different Young tableau in Eqs. (14) and (17) are the same in a tensor form. We define the color singlets derived from the above methods, as follows:

$$|C_1\rangle = [\{(12)_6(34)_{\bar{3}}\}_3 5_{\bar{3}}]_1 = [\{(12)_6 3\}_8(45)_8]_1,$$
$$|C_2\rangle = [\{(12)_{\bar{3}}34\}_3 5_{\bar{3}}]_1 = [\{(12)_{\bar{3}}3\}_8(45)_8]_1,$$
$$|C_3\rangle = [\{(123)_1 4\}_3 5_{\bar{3}}]_1 = [\{(123)_1(45)_1]_1. \tag{18}$$

C. Spin states

For the spin $= 3/2$ pentaquark case, the spin states are represented in terms of Young tableau [41] with four dimensions, as follows:

$$|S_1^{3/2}\rangle = \begin{array}{|c|c|c|c|}\hline 1&2&3&4\\\hline 5\\\cline{1-1}\end{array},\ |S_2^{3/2}\rangle = \begin{array}{|c|c|c|c|}\hline 1&2&3&5\\\hline 4\\\cline{1-1}\end{array},\ |S_3^{3/2}\rangle = \begin{array}{|c|c|c|c|}\hline 1&2&4&5\\\hline 3\\\cline{1-1}\end{array},$$
$$|S_4^{3/2}\rangle = \begin{array}{|c|c|c|c|}\hline 1&3&4&5\\\hline 2\\\cline{1-1}\end{array}. \tag{19}$$

When we investigate the stability of the pentaquark against the strong decay into a baryon and a meson, it is very convenient to use the spin states related with the decay mode. We denote the four spin states by

$$|\phi_1\rangle = [\{(12)_1 3_{1/2}\}_{3/2}(45)_0]_{3/2},$$
$$|\phi_2\rangle = [\{(12)_1 3_{1/2}\}_{3/2}(45)_1]_{3/2},$$
$$|\phi_3\rangle = [\{(12)_1 3_{1/2}\}_{1/2}(45)_1]_{3/2},$$
$$|\phi_4\rangle = [\{(12)_0 3_{1/2}\}_{1/2}(45)_1]_{3/2}, \tag{20}$$

where the subscript indicates the spin state. Because of the orthonormality of the two sets of spin sates, Eqs. (19) and (20) are related by the following orthogonal transformation:

$$\begin{pmatrix} \sqrt{\frac{5}{8}} & \sqrt{\frac{3}{8}} & 0 & 0 \\ -\sqrt{\frac{3}{8}} & \sqrt{\frac{5}{8}} & 0 & 0 \\ 0 & 0 & 1 & 0 \\ 0 & 0 & 0 & 1 \end{pmatrix}. \tag{21}$$

D. Isospin ⊗ color ⊗ spin state for $I = 1/2$

Since the isospin, color, and spin states represented in terms of the Young tableau have a certain symmetry property, we can construct the isospin ⊗ color ⊗ spin state of the pentaquark that is fully antisymmetric under the exchange of any pair among particles 1–3. For this purpose, depending on how the coupling scheme is implemented, we consider two methods. In the first method, we start from the notation of the color singlets in Eq. (14), and combine the color singlets with spin states by the out-product of the permutation group, S_4, resulting in the color ⊗ spin states for particles 1–4. Then, we can easily obtain the isospin ⊗ color ⊗ spin state with $\{123\}$ symmetry by coupling the isospin state with the color ⊗ spin states. In the second method, we start the notation of the color singlets in Eq. (17), and use the S_3 permutation group applied on the coupling scheme.

According to the permutation group theory [30], the irreducible basis of S_5 becomes the irreducible basis of S_4 as well, irrespective of particle 5. When we consider the symmetry property for particles 1–4 in coupling scheme, we can identify the spin states in Eq. (19) with the Young-Yamanouchi bases for the Young tableau [4] and Young tableau [31] without particle 5,

$$|S_1^{3/2}\rangle = \begin{array}{|c|c|c|c|}\hline 1&2&3&4\\\hline\end{array},\ |S_2^{3/2}\rangle = \begin{array}{|c|c|c|}\hline 1&2&3\\\hline 4\\\cline{1-1}\end{array},\ |S_3^{3/2}\rangle = \begin{array}{|c|c|c|}\hline 1&2&4\\\hline 3\\\cline{1-1}\end{array},$$
$$|S_4^{3/2}\rangle = \begin{array}{|c|c|c|}\hline 1&3&4\\\hline 2\\\cline{1-1}\end{array}. \tag{22}$$

It is necessary to show the inner product between the Young tableau [211] of the color singlets in Eq. (14) and Young tableau [31] of the spin states in Eq. (22) so that we obtain the color ⊗ spin states,

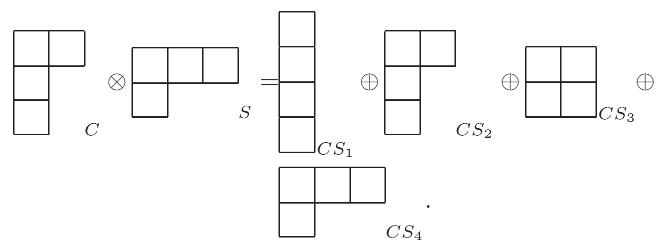

(23)

In addition to this, we should consider the inner product between the Young tableau [211] of the color singlets in Eq. (14) and Young tableau [4] of the spin states in Eq. (22),

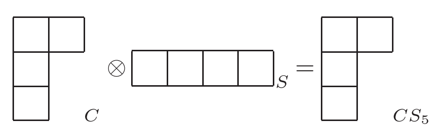

(24)

The coupling scheme designed to construct the isospin ⊗ color ⊗ spin states with the $\{123\}$ symmetry is completed by using the Clebsch-Gordan (CG) coefficient of the permutation group, S_n, which is factorized into the CG coefficient of S_{n-1} and K matrix [31], given by

$$S([f']p'q'y'[f'']p''q''y''|[f]pqy) = K([f']p'[f'']p''|[f]p)S([f'_{p'}]q'y'[f''_{p''}]q''y''|[f_p]qy), \tag{25}$$

where S in the left-hand (right-hand) side is a CG coefficient of S_n (S_{n-1}). In this work, we take a similar process as described in Refs. [29,32].

Below, we show the Young-Yamanouchi bases corresponding to the Young tableau [211] that is obtained from the color ⊗ spin coupling in Eq. (23),

$$\begin{array}{|c|c|}\hline 1&2\\\hline 3\\\cline{1-1} 4\\\cline{1-1}\end{array}_{CS_2} = -\frac{1}{\sqrt{6}}|C_1\rangle\otimes|S_2^{3/2}\rangle - \frac{1}{\sqrt{3}}|C_1\rangle\otimes|S_3^{3/2}\rangle + \frac{1}{\sqrt{3}}|C_2\rangle\otimes|S_4^{3/2}\rangle - \frac{1}{\sqrt{6}}|C_3\rangle\otimes|S_4^{3/2}\rangle. \tag{26}$$

$$\begin{array}{|c|c|}\hline 1&3\\\hline 2\\\cline{1-1} 4\\\cline{1-1}\end{array}_{CS_2} = \frac{1}{\sqrt{3}}|C_1\rangle\otimes|S_4^{3/2}\rangle - \frac{1}{\sqrt{6}}|C_2\rangle\otimes|S_2^{3/2}\rangle + \frac{1}{\sqrt{3}}|C_2\rangle\otimes|S_3^{3/2}\rangle + \frac{1}{\sqrt{6}}|C_3\rangle\otimes|S_3^{3/2}\rangle. \tag{27}$$

For the case of the Young tableau [22], which is obtained from the color ⊗ spin coupling in Eq. (23), the Young-Yamanouchi bases are as follows:

$$\begin{array}{|c|c|}\hline 1&2\\\hline 3&4\\\hline\end{array}_{CS_3} = -\frac{1}{\sqrt{3}}|C_1\rangle\otimes|S_2^{3/2}\rangle + \frac{1}{\sqrt{6}}|C_1\rangle\otimes|S_3^{3/2}\rangle - \frac{1}{\sqrt{6}}|C_2\rangle\otimes|S_4^{3/2}\rangle - \frac{1}{\sqrt{3}}|C_3\rangle\otimes|S_4^{3/2}\rangle. \tag{28}$$

$$\begin{array}{|c|c|}\hline 1&3\\\hline 2&4\\\hline\end{array}_{CS_3} = -\frac{1}{\sqrt{6}}|C_1\rangle\otimes|S_4^{3/2}\rangle - \frac{1}{\sqrt{3}}|C_2\rangle\otimes|S_2^{3/2}\rangle - \frac{1}{\sqrt{6}}|C_2\rangle\otimes|S_3^{3/2}\rangle + \frac{1}{\sqrt{3}}|C_3\rangle\otimes|S_3^{3/2}\rangle. \tag{29}$$

For the case of the Young tableau [31], which is obtained from the color ⊗ spin coupling in Eq. (23), the Young-Yamanouchi bases are as follows:

$$\begin{array}{|c|c|c|}\hline 1&2&4\\\hline 3\\\cline{1-1}\end{array}_{CS_4} = -\frac{1}{\sqrt{2}}|C_1\rangle\otimes|S_2^{3/2}\rangle + \frac{1}{\sqrt{2}}|C_3\rangle\otimes|S_4^{3/2}\rangle. \tag{30}$$

$$\begin{array}{|c|c|c|}\hline 1&3&4\\\hline 2\\\cline{1-1}\end{array}_{CS_4} = -\frac{1}{\sqrt{2}}|C_2\rangle\otimes|S_2^{3/2}\rangle - \frac{1}{\sqrt{2}}|C_3\rangle\otimes|S_3^{3/2}\rangle. \tag{31}$$

For the case of the Young tableau [211], which is obtained from the color ⊗ spin coupling in Eq. (24), the Young-Yamanouchi bases are as follows:

$$\begin{array}{|c|c|}\hline 1&2\\\hline 3\\\cline{1-1} 4\\\cline{1-1}\end{array}_{CS_5} = |C_1\rangle\otimes|S_1^{3/2}\rangle. \tag{32}$$

$$\begin{array}{|c|c|}\hline 1&3\\\hline 2\\\cline{1-1} 4\\\cline{1-1}\end{array}_{CS_5} = |C_2\rangle\otimes|S_1^{3/2}\rangle. \tag{33}$$

To find the isospin ⊗ color ⊗ spin state with $\{123\}$ symmetry, we finally combine the isospin states in Eq. (12) with color ⊗ spin states for the Young tableau [211] in Eq. (24) as well as the Young tableau [211], [22], and [31] in Eq. (23). Therefore, we have four isospin ⊗ color ⊗ spin states with $\{123\}$ symmetry for $I = 1/2$,

$$\begin{aligned}
|[I^{\frac{1}{2}}CS]_1\rangle &= \frac{1}{\sqrt{2}}\left(\begin{array}{|c|c|}\hline 1&2\\\hline 3\\\cline{1-1}\end{array}_{I}\otimes\begin{array}{|c|c|}\hline 1&3\\\hline 2\\\cline{1-1} 4\\\cline{1-1}\end{array}_{CS_2} - \begin{array}{|c|c|}\hline 1&3\\\hline 2\\\cline{1-1}\end{array}_{I}\otimes\begin{array}{|c|c|}\hline 1&2\\\hline 3\\\cline{1-1} 4\\\cline{1-1}\end{array}_{CS_2}\right)\\
|[I^{\frac{1}{2}}CS]_2\rangle &= \frac{1}{\sqrt{2}}\left(\begin{array}{|c|c|}\hline 1&2\\\hline 3\\\cline{1-1}\end{array}_{I}\otimes\begin{array}{|c|c|}\hline 1&3\\\hline 2&4\\\hline\end{array}_{CS_3} - \begin{array}{|c|c|}\hline 1&3\\\hline 2\\\cline{1-1}\end{array}_{I}\otimes\begin{array}{|c|c|}\hline 1&2\\\hline 3&4\\\hline\end{array}_{CS_3}\right)\\
|[I^{\frac{1}{2}}CS]_3\rangle &= \frac{1}{\sqrt{2}}\left(\begin{array}{|c|c|}\hline 1&2\\\hline 3\\\cline{1-1}\end{array}_{I}\otimes\begin{array}{|c|c|c|}\hline 1&3&4\\\hline 2\\\cline{1-1}\end{array}_{CS_4} - \begin{array}{|c|c|}\hline 1&3\\\hline 2\\\cline{1-1}\end{array}_{I}\otimes\begin{array}{|c|c|c|}\hline 1&2&4\\\hline 3\\\cline{1-1}\end{array}_{CS_4}\right)\\
|[I^{\frac{1}{2}}CS]_4\rangle &= \frac{1}{\sqrt{2}}\left(\begin{array}{|c|c|}\hline 1&2\\\hline 3\\\cline{1-1}\end{array}_{I}\otimes\begin{array}{|c|c|}\hline 1&3\\\hline 2\\\cline{1-1} 4\\\cline{1-1}\end{array}_{CS_5} - \begin{array}{|c|c|}\hline 1&3\\\hline 2\\\cline{1-1}\end{array}_{I}\otimes\begin{array}{|c|c|}\hline 1&2\\\hline 3\\\cline{1-1} 4\\\cline{1-1}\end{array}_{CS_5}\right).
\end{aligned} \tag{34}$$

Here and in the next two equations, we have neglected the explicit notation of particle 4 (and 5) as we are only interested in the symmetry properties of particles 1–3. From the notation of the color singlets in Eq. (17), which represents the symmetry of the permutation group, S_3, we easily see that the $|C_3\rangle$ state has the symmetry property with $\{123\}$. For that reason, the isospin ⊗ spin state in combining with the $|C_3\rangle$ state should be fully symmetric in the exchange of any pair among particles 1–3, and the coupling of the $|C_3\rangle$ state with the isospin ⊗ spin states gives the isospin ⊗ color ⊗ spin state with $\{123\}$ symmetry. We denote the isospin ⊗ spin states satisfying fully symmetry by

$$\begin{array}{|c|c|c|}\hline 1&2&3\\\hline\end{array}_{IS} = \frac{1}{\sqrt{2}}\left(\begin{array}{|c|c|}\hline 1&2\\\hline 3\\\cline{1-1}\end{array}_{I}\otimes\begin{array}{|c|c|c|c|}\hline 1&2&4&5\\\hline 3\\\cline{1-1}\end{array}_{S} + \begin{array}{|c|c|}\hline 1&3\\\hline 2\\\cline{1-1}\end{array}_{I}\otimes\begin{array}{|c|c|c|c|}\hline 1&3&4&5\\\hline 2\\\cline{1-1}\end{array}_{S}\right). \tag{35}$$

On the contrary, since both $|S_1^{3/2}\rangle$ and $|S_2^{3/2}\rangle$ sates in Eq. (19) are fully symmetric in the exchange of any pair among particles 1–3, the isospin ⊗ color state in combining with either the $|S_1^{3/2}\rangle$ or $|S_2^{3/2}\rangle$ state should have the opposite symmetry for the same reason. We denote the isospin ⊗ color state satisfying full antisymmetry by

$$\young(1,2,3)_{IC} = \frac{1}{\sqrt{2}}\left(\young(12,3)_I \otimes \young(13,2)_8 \otimes (45)_8 - \young(13,2)_I \otimes \young(12,3)_8 \otimes (45)_8 \right). \tag{36}$$

Lastly, we can consider the color $\otimes$ spin states corresponding to the Young tableau that are conjugate to that of the isospin states, for the reason that any fully antisymmetric state can be obtained by the coupling of any Young tableau with the conjugate. We denote the color $\otimes$ spin states corresponding to the Young tableau [21] for particles 1–3 by

$$\begin{aligned} \young(12,3)_{CS} &= \frac{1}{\sqrt{2}}\left(\young(12,3)_8 \otimes (45)_8 \otimes \young(1245,3)_S - \young(13,2)_8 \otimes (45)_8 \otimes \young(1345,2)_S \right), \\ \young(13,3)_{CS} &= -\frac{1}{\sqrt{2}}\left(\young(12,3)_8 \otimes (45)_8 \otimes \young(1345,2)_S + \young(13,2)_8 \otimes (45)_8 \otimes \young(1245,3)_S \right). \end{aligned} \tag{37}$$

We denote another set of the isospin $\otimes$ color $\otimes$ spin states satisfying full symmetry by

$$\begin{aligned} |\psi_1\rangle &= |C_3\rangle \otimes \young(123)_{IS}, \quad |\psi_2\rangle = \young(1,2,3)_{IC} \otimes \young(1235,4)_S, \\ |\psi_3\rangle &= \frac{1}{\sqrt{2}}\left(\young(12,3)_I \otimes \young(13,2)_{CS} - \young(13,2)_I \otimes \young(12,3)_{CS} \right), \\ |\psi_4\rangle &= \young(1,2,3)_{IC} \otimes \young(1234,5)_S. \end{aligned} \tag{38}$$

We note that both the states in Eq. (34) and the states in Eq. (38) are orthonormal to each other in four-dimensional vector space, respectively.

It is worthwhile to mention that from a hadron state point of view $|\psi_1\rangle$ accounts for the $(p)_1 \otimes (J/\psi)_1$ state, where the subscript indicates the color state; in fact the color part consists of the color singlet of a baryon multiplied by the color singlet of a meson, and the spin part contains a baryon with spin $= 1/2$ multiplied by a meson with spin $= 1$ in Eq. (21). On the other hand, $|\psi_2\rangle$ represents the $(p)_8 \otimes (J/\psi)_8$ state, namely coming from the color octet of a baryon multiplied by the color octet of a meson. By rearranging the quarks, one can also represent this state as a linear combination of a charmed baryon and meson state as we show in Appendix C.

In a vector space with four dimensions where the isospin $\otimes$ color $\otimes$ spin states have the symmetry property with $\{123\}$, there exists an orthogonal matrix that transforms the set of Eq. (38) into the set of Eq. (34), given by

$$\begin{pmatrix} \frac{1}{\sqrt{6}} & \frac{1}{\sqrt{3}} & -\frac{1}{\sqrt{2}} & 0 \\ -\frac{1}{\sqrt{6}} & -\frac{1}{\sqrt{3}} & -\frac{1}{\sqrt{2}} & 0 \\ -\frac{\sqrt{2}}{\sqrt{3}} & -\frac{1}{\sqrt{3}} & 0 & 0 \\ 0 & 0 & 0 & 1 \end{pmatrix}. \tag{39}$$

IV. NUMERICAL RESULTS

In this section, we analyze the numerical results performed using the variational method for the Hamiltonian given in Eq. (1). For that purpose, we adopt the trial wave function that consists of the spatial function in Eq. (9) and the isospin $\otimes$ color $\otimes$ spin states obtained from Sec. III. The trial wave function can thus be expanded as follows:

$$|\Psi_\alpha\rangle = \sum_i C_i^\alpha |R\rangle |[ICS]_i\rangle. \tag{40}$$

Before discussing the numerical analysis, it is useful to examine the expectation value of the color spin part of the hyperfine potential, with the spatial dependence factored out, in the matrix form generated by the four independent isospin $\otimes$ color $\otimes$ spin states. This hyperfine matrix is essential in identifying possible attraction in the four configurations. A stable or resonant pentaquark state can only exist if the hyperfine potential of the pentaquark configuration is sufficiently attractive compared to that from the sum of a baryon and a meson. The 4 by 4 matrix form of the expectation value of the hyperfine factor of the pentaquark configuration generated by the isospin $\otimes$ color $\otimes$ spin states in Eq. (34) is given as follows:

$$-\left\langle \sum_{i<j}^{5} \frac{1}{m_i m_j} \lambda_i^c \lambda_j^c \sigma_i \cdot \sigma_j \right\rangle = \begin{pmatrix} -\frac{7}{3m_1^2}+\frac{1}{2m_2^2}+\frac{19}{6m_1m_2} & -\frac{\sqrt{2}}{3m_1^2}+\frac{7}{3\sqrt{2}m_2^2}-\frac{5\sqrt{2}}{6m_1m_2} & \frac{5}{\sqrt{3}m_1^2}-\frac{5}{2\sqrt{3}m_2^2}-\frac{5}{2\sqrt{3}m_1m_2} & \frac{\sqrt{5}}{3\sqrt{2}m_2^2}+\frac{23\sqrt{5}}{3\sqrt{2}m_1m_2} \\ -\frac{\sqrt{2}}{3m_1^2}+\frac{7}{3\sqrt{2}m_2^2}-\frac{5\sqrt{2}}{6m_1m_2} & -\frac{8}{3m_1^2}+\frac{5}{3m_2^2}+\frac{7}{3m_1m_2} & \frac{5\sqrt{2}}{\sqrt{3}m_1^2}-\frac{5}{\sqrt{6}m_2^2}-\frac{5}{\sqrt{6}m_1m_2} & \frac{\sqrt{5}}{3m_2^2}-\frac{\sqrt{5}}{3m_1m_2} \\ \frac{5}{\sqrt{3}m_1^2}-\frac{5}{2\sqrt{3}m_2^2}-\frac{5}{2\sqrt{3}m_1m_2} & \frac{5\sqrt{2}}{\sqrt{3}m_1^2}-\frac{5}{\sqrt{6}m_2^2}-\frac{5}{\sqrt{6}m_1m_2} & -\frac{3}{m_1^2}+\frac{17}{6m_2^2}-\frac{13}{2m_1m_2} & \frac{\sqrt{5}}{\sqrt{6}m_2^2}-\frac{\sqrt{5}}{\sqrt{6}m_1m_2} \\ \frac{\sqrt{5}}{3\sqrt{2}m_2^2}+\frac{23\sqrt{5}}{3\sqrt{2}m_1m_2} & \frac{\sqrt{5}}{3m_2^2}-\frac{\sqrt{5}}{3m_1m_2} & \frac{\sqrt{5}}{\sqrt{6}m_2^2}-\frac{\sqrt{5}}{\sqrt{6}m_1m_2} & \frac{2}{m_1^2}+\frac{1}{m_2^2}-\frac{3}{m_1m_2} \end{pmatrix}. \tag{41}$$

TABLE III. The sum of the expectation value of the hyperfine factor of both a baryon and a meson for the possible decay channel with respect to $I = 1/2$. The third column shows the value for the fitting mass m_u and m_c [in units $(\mathrm{GeV})^{-2}$].

Decay channel	$-\langle \sum_{i<j}^{N} \frac{1}{m_i m_j} \lambda_i^c \lambda_j^c \sigma_i \cdot \sigma_j \rangle$	Value
pJ/ψ	$-\frac{8}{m_1{}^2} + \frac{16}{3m_2{}^2}$	−86.2
$\Lambda_c D^*$	$-\frac{8}{m_1{}^2} + \frac{16}{3m_1 m_2}$	−78.3
$\Sigma_c^* D$	$\frac{8}{3m_1{}^2} - \frac{32}{3m_1 m_2}$	10.5
$\Sigma_c D^*$	$\frac{8}{3m_1{}^2} - \frac{16}{3m_1 m_2}$	19.8
$\Sigma_c^* D^*$	$\frac{8}{3m_1{}^2} + \frac{32}{3m_1 m_2}$	47.9

To compare the expectation values of the hyperfine factor of the pentaquark with the corresponding sum of a baryon and a meson, we need to diagonalize $-\langle \sum_{i<j}^{5} \frac{1}{m_i m_j} \lambda_i^c \lambda_j^c \sigma_i \cdot \sigma_j \rangle$ in Eq. (41) and compare it to the possible decay channels. The diagonalized form of the matrix $-\langle \sum_{i<j}^{5} \frac{1}{m_i m_j} \lambda_i^c \lambda_j^c \sigma_i \cdot \sigma_j \rangle$ in Eq. (41) can be represented as combinations of terms proportional to $1/m_1{}^2$, $1/m_2{}^2$, and $1/(m_1 m_2)$, respectively. When the fitting mass m_u and m_c in Table I is used, the ground state is given as

$$-\frac{7.88}{m_1{}^2} + \frac{5.29}{m_2{}^2} - \frac{1.41}{m_1 m_2} = -87.3\ (\mathrm{GeV})^{-2}. \qquad (42)$$

As can be seen in Table III, the ground state of the diagonalized hyperfine factor of the pentaquark in Eq. (42) is slightly more attractive than the most attractive $p + J/\psi$ decay channel. This attraction is coming from the term proportional to $1/m_1 m_2$, which originates from the additional attraction coming from bringing the color octet component of p and J/ψ together, as noted recently in Ref. [24]. However, as we show below, the attraction is very small and does not compensate for the additional kinetic energy term that arises from making the pentaquark state compact compared to the isolated meson baryon states.

To investigate the mass and the property of the pentaquark with the variational method, we calculate the Schrödinger equation $H|\Psi_\alpha\rangle = E_\alpha|\Psi_\alpha\rangle$ and diagonalize the 4×4 matrix. We find the ground state to be 4087.6 MeV, which is the sum of the mass of the p and J/ψ in our model. The wave function is given as

$$|\Psi_g\rangle = -0.4082|R\rangle|[I^{\frac{1}{2}}CS]_1\rangle - 0.5773|R\rangle|[I^{\frac{1}{2}}CS]_2\rangle + 0.7071|R\rangle|[I^{\frac{1}{2}}CS]_3\rangle, \qquad (43)$$

where the variational parameters are given as $a_1 = 3.4\ \mathrm{fm}^{-2}$, $a_2 = 1.4\ \mathrm{fm}^{-2}$, $a_3 = 11\ \mathrm{fm}^{-2}$, and $a_4 \sim 0$. The first two parameters and the third parameter correspond to those of the baryon and meson, respectively, while the last shows that the distance between the center of mass of the baryon and the meson approaches infinity. In fact, as we can see from the transformation matrix in Eq. (39), the ground state, $|\Psi_g\rangle$, for $I = 1/2$ is exactly equal to $-(p)_1 \otimes (J/\psi)_1$ corresponding to $|\psi_1\rangle$ in Eq. (38), which means that the ground state corresponds to the isolated p and J/ψ state in the relative S wave.

It is useful to inspect the expectation value of the Hamiltonian for the state $|\psi_1\rangle$ to understand why the separated p and J/ψ configuration becomes the ground state. First, the hyperfine potential $-\langle \sum_{i<j}^{5} \frac{1}{m_i m_j} \lambda_i^c \lambda_j^c \sigma_i \cdot \sigma_j \rangle$ is $-\frac{8}{m_1{}^2} + \frac{16}{3m_2{}^2}$, which is exactly equal to the sum of the expectation value of the p and J/ψ with the first term (the second) coming from the p (J/ψ). Moreover, as discussed before, the lowest eigenvalue of the hyperfine matrix is not so different from this value, suggesting that the attraction in the color octet p and J/ψ is not so strong. As for the confinement potential, as can be seen from Eqs. (A1) and (A2) in the appendix, the first diagonal components consist of the terms corresponding to the p and J/ψ only. Therefore, the only mass difference between the pentaquark and the $p + J/\psi$ channel comes from the additional kinetic term, which vanishes for the separated $p + J/\psi$ state. Using the last term in Eq. (10), one can estimate the additional kinetic energy to bring the p and J/ψ together. Taking $a_4 \sim 2\ \mathrm{fm}^{-2}$, which corresponds to a separation of about 0.7 fm, one obtains an extra kinetic energy of 200 MeV, making the energy of the compact pentaquark state around 4290 MeV. Even if we allow the other three states to mix, which could bring in small additional hyperfine attraction, the additional confining potential will conspire to keep the $(p)_1 \otimes (J/\psi)_1$ state the dominant compact configuration. Obviously, such a compact state would just fall apart into the $p + J/\psi$ state and thus not be stable unless the spatial wave function has a small overlap with the final state $p + J/\psi$ [33].

As any configuration generated with $|\psi_1\rangle$ is dominated by the fall apart $p + J/\psi$ state, we need to investigate whether the excited state can be compact and quasistable. To accomplish this, we consider the $|\psi_2\rangle$, $|\psi_3\rangle$, and $|\psi_4\rangle$ in Eq. (38) without $|\psi_1\rangle$. The detailed property of the excited state of this state is given in Table IV. Because of the quantum numbers, except for the $p + J/\psi$ configuration, the excited states cannot be written as a sum of a single baryon and meson state. Hence, we find a compact state. However, it can decay into several baryon and meson decay channels and is not stable. As for the color spin part of the potential $-\langle \sum_{i<j}^{5} \frac{1}{m_i m_j} \lambda_i^c \lambda_j^c \sigma_i \cdot \sigma_j \rangle$, we find that this state has the following form:

$$-\frac{1.27}{m_1{}^2} - \frac{0.45}{m_2{}^2} - \frac{5.38}{m_1 m_2} = -23.4\ (\mathrm{GeV})^{-2}. \qquad (44)$$

While the diagonalized hyperfine factor is less attractive than that of the $p + J/\psi$ and $\Lambda_c + D^*$ decay channels, it is still more attractive than other decay channels. Nevertheless,

TABLE IV. The mass of the excited state of the pentaquark with $I = 1/2$ obtained from the variational method, by diagonalizing the matrix element of the Hamiltonian in terms of $|R\rangle|\psi_2\rangle$, $|R\rangle|\psi_3\rangle$, and $|R\rangle|\psi_4\rangle$. Δ_B indicate the binding energy. The units for the energy and variational parameter are GeV and fm^{-2}, respectively.

I = 1/2	$q^3c\bar{c}$				
Mass	4.626				
Variational parameters	$a_1 = 2.3,\ a_2 = 1.4,\ a_3 = 4,\ a_2 = 3.4$				
Decay channel	pJ/ψ	$\Lambda_c D^*$	$\Sigma_c^* D$	$\Sigma_c D^*$	$\Sigma_c^* D^*$
Threshold	4.088	4.298	4.408	4.471	4.548
Δ_B	0.538	0.328	0.218	0.155	0.078

the reason why the excited state has energy larger than any decay channel is due to the large contribution from the confining potential. As discussed in the appendix, the sum of the color matrix is all equal for the four orthonormal states. However, due to the interplay with the kinetic term, the confining part of the potential is most attractive in the $p + J/\psi$ channel. The contributions from the kinetic, confinement, and hyperfine interaction terms for the excited pentaquark state as well as separated baryon meson states are summarized in Table V. The large confinement contribution for the pentaquark state can be seen in Table V. The obtained mass is too large for it to be one of the recently observed pentaquark states. Moreover, it will decay to all possible baryon meson states and not be stable.

V. SUMMARY

To understand the possible quark configuration of the recently observed hidden charm pentaquark state, we systematically construct the isospin ⊗ color ⊗ spin pentaquark states containing two heavy quarks and antiquarks with $I = 1/2$ and $S = 3/2$ that satisfy the Pauli principle. We systematically derive the isospin ⊗ color ⊗ spin states from the color and spin coupling scheme, which is based on the permutation group property. We found that there are four orthonormal states, one of which is the color, spin, and isospin corresponding to the proton and J/ψ. Then, by using a spatial trial wave function that is suitable for describing the decay into a baryon and meson state, we perform the variational method to obtain the lowest mass state of the pentaquark with $I = 1/2$ and $S = 3/2$. We found that the ground state is the isolated $p + J/\psi$ state and that the compact configuration with the lowest energy is also dominated by the same baryon and meson state, which will thus fall apart or decay to the ground state. We further calculate the mass with an excited state, involving the other isospin ⊗ color ⊗ spin states that are orthonormal to the ground state. The mass of the compact excited state is found to be well above all baryon meson decay channels and not stable. We are therefore led to conclude that the recently observed pentaquark state cannot be a compact multiquark state within the conventional constituent quark model with only confining and color spin interaction. There could still be intrinsic three- or four-body quark interaction that might change the situation. A flux-tube inspired configuration leading to a confinement different from those used in the additive rule in Eq. (1) may increase the stability of pentaquarks.

As we discuss in Appendix C, it should be noted that all the discussion based on the color basis can be recast into a basis composed of color singlet baryon-meson basis. In fact, if there were any additional strong attraction due to color interaction from bringing all the quarks together, such an effect should also be present in the baryon-meson basis. In this work, we chose to probe such a possibility in terms of the conventional quark interaction that should be valid typically only up to distances of normal hadrons. If the state is a resonance of larger size or a hadronic bound state, such as the deuteron, our approach will certainly not be able to probe. A minimal extension of our approach to probe such a configuration has to include interactions involving pions and/or other mesons, which could be a topic for future works.

TABLE V. The values of each energy term of the excited state of the pentaquark and the sum of a baryon and a meson in the decay channel. ΔE is the difference between the pentaquark and its decay channel in each term (units in MeV).

Pentaquark	Kinetic	Comfinement	Hyperfine
The excited state	1144.3	1238	−52.1
Decay channel	Kinetic	Comfinement	Hyperfine
pJ/ψ	1190.5	745.8	−145.1
ΔE	−46.2	492.2	93
$\Lambda_c D^*$	1192.7	982.2	−173.1
ΔE	−48.4	255.8	121
$\Sigma_c^* D$	1105.3	1055.1	−48.6
ΔE	39	182.9	−3.5
$\Sigma_c D^*$	1046.5	1102.9	25.8
ΔE	97.8	135.1	−77.9
$\Sigma_c^* D^*$	993.1	1157	101.4
ΔE	151.2	81	−153.5

ACKNOWLEDGMENTS

This work was supported by the Korea National Research Foundation (NRF) under Grant No. 2016R1D1A1B03930089. The work of W. S. P. was supported in part by the Yonsei University Research Fund (Postdoctoral Researcher Supporting Program) of 2014 (Grant No. 2014-12-0139). The work of S. C. and W. S. P. was supported by the NRF grant funded by the Korea government (MSIP) (Grant No. 2016R1C1B1016270).

APPENDIX A: THE MATRIX ELEMENT OF $\lambda_i^c\lambda_j^c$

In Appendix A, we present the matrix element of $\lambda_i^c\lambda_j^c$ $(i < j = 1 \sim 5)$ of the pentaquark in terms of a four-dimensional matrix generated by the states $|\psi_1\rangle$, $|\psi_2\rangle$, $|\psi_3\rangle$, and $|\psi_4\rangle$ in Eq. (38).

(a) $(i,j) = (1,2)$, (1,3), or (2,3),

$$\langle \lambda_i^c \lambda_j^c \rangle = \begin{pmatrix} -\frac{8}{3} & 0 & 0 & 0 \\ 0 & -\frac{2}{3} & 0 & 0 \\ 0 & 0 & -\frac{2}{3} & 0 \\ 0 & 0 & 0 & -\frac{2}{3} \end{pmatrix}, \quad \text{(A1)}$$

(b) $(i,j) = (1,4)$, (1,5), (2,4), (2,5), (3,4), or (3,5),

$$\langle \lambda_i^c \lambda_j^c \rangle = \begin{pmatrix} 0 & 0 & 0 & 0 \\ 0 & -2 & 0 & 0 \\ 0 & 0 & -2 & 0 \\ 0 & 0 & 0 & -2 \end{pmatrix}, \quad \text{(A2)}$$

(c) $(i,j) = (4,5)$,

$$\langle \lambda_i^c \lambda_j^c \rangle = \begin{pmatrix} -\frac{16}{3} & 0 & 0 & 0 \\ 0 & \frac{2}{3} & 0 & 0 \\ 0 & 0 & \frac{2}{3} & 0 \\ 0 & 0 & 0 & \frac{2}{3} \end{pmatrix}. \quad \text{(A3)}$$

It is easily seen that $\langle \sum_{i<j}^5 \lambda_i^c \lambda_j^c \rangle = -40/3I$, where the I is the identity matrix.

In the case of a baryon, $\langle \sum_{i<j}^3 \lambda_i^c \lambda_j^c \rangle = -8$ coming from the color singlet state $\frac{1}{\sqrt{6}} \epsilon_{ijk} q^i(1) q^j(2) q^k(3))$. For a meson state, $\langle \lambda_4^c \lambda_5^c \rangle = -16/3$ with the color state $\bar{q}_i(4) q^i(5)$. These values are the first diagonal components in the above matrix elements. Hence, as pointed out before, we find that the first diagonal term of $\langle \sum_{i<j}^5 \lambda_i^c \lambda_j^c \rangle$ of the pentaquark is just the sum of those of the baryon and meson. In fact, as far as this color matrix is concerned, all the four sums of the diagonal matrix elements have the same value. However, depending on the spatial wave function, the matrices for the confining potential have different weighting factors coming from spatial wave functions and their sum is no longer proportional to the identity matrix. If the kinetic terms are considered, it is energetically more favorable to maximize the attraction in the p and J/ψ channel, which makes it the most attractive state even for compact configurations.

APPENDIX B: THE COLOR SINGLETS OF THE PENTAQUARK

In Appendix B, we present the tensor form for the color singlet states of the pentaquark, and prove Eq. (18). We can first represent the Young-Yamanuchi bases of the Young tableau [211] in Eq. (13) as a rank (1,0) tensor. First, one notes that

$$\{(123)_1 4\}_3 = \frac{1}{\sqrt{6}} \epsilon^{lmn} q_l(1) q_m(2) q_n(3) q_i(4). \quad \text{(B1)}$$

Then, using the well-known relation between Young-Yamanuchi bases, we can obtain the other Young-Yamanuchi basis for the Young tableau [211],

$$\{(12)_{\bar{3}} 34\}_3 = \frac{3}{\sqrt{8}} \left[(34) \{(123)_1 4\}_3 - \frac{1}{3} \{(123)_1 4\}_3 \right],$$
$$\{(12)_6 (34)_{\bar{3}}\}_3 = \frac{2}{\sqrt{3}} \left[(23) \{(12)_{\bar{3}} 34\}_3 - \frac{1}{2} \{(12)_{\bar{3}} 34\}_3 \right], \quad \text{(B2)}$$

where (34) and (23) are the permutation operators. We represent the $\{(12)_{\bar{3}} 34\}_3$ and $\{(12)_6 (34)_{\bar{3}}\}_3$ as follows:

$$\{(12)_{\bar{3}} 34\}_3 = \frac{\sqrt{3}}{4} \left[\epsilon^{lmn} q_l(1) q_m(2) q_n(4) q_i(3) - \frac{1}{3} \epsilon^{lmn} q_l(1) q_m(2) q_n(3) q_i(4) \right],$$
$$\{(12)_6 (34)_{\bar{3}}\}_3 = \frac{1}{4} [\epsilon^{lmn} q_l(1) q_m(3) q_n(4) q_i(2) + \epsilon^{lmn} q_l(2) q_m(2) q_n(4) q_i(1)]. \quad \text{(B3)}$$

In calculating the $\{(12)_6 (34)_{\bar{3}}\}_3$ we utilize the useful formula, given by

$$\epsilon^{lmn} q_l(1) q_m(2) q_n(3) q_i(4) - \epsilon^{lmn} q_l(1) q_m(2) q_n(4) q_i(3) = -\epsilon^{lmn} q_l(1) q_m(3) q_n(4) q_i(2) + \epsilon^{lmn} q_l(2) q_m(3) q_n(4) q_i(1). \quad \text{(B4)}$$

It is easily seen that $\{(12)_{\bar{3}} 34\}_3$ is antisymmetric under the exchange of particles 1 and 2, while $\{(12)_6 (34)_{\bar{3}}\}_3$ is symmetric (antisymmetric) under the exchange of particles 1 and 2 (particles 3 and 4).

Finally, we can obtain the three color singlets of the pentaquark, which are orthogonal to each other, by combining $\{(123)_1 4\}_3$, $\{(12)_{\bar{3}} 34\}_3$, and $\{(12)_6 (34)_{\bar{3}}\}_3$ with $\bar{q}^i(5)$, a rank (0,1) tensor, through contraction and normalization. These are given as

$$\begin{aligned}
[\{(12)_6(34)_{\bar{3}}\}_3 5_{\bar{3}}]_1 &= \frac{1}{4\sqrt{3}}[\epsilon^{lmn}q_l(1)q_m(3)q_n(4)q_i(2)\bar{q}^i(5) \\
&\quad + \epsilon^{lmn}q_l(2)q_m(3)q_n(4)q_i(1)\bar{q}^i(5)] \\
&= |C_1\rangle, \\
[\{(12)_{\bar{3}}34\}_3 5_{\bar{3}}]_1 &= \frac{1}{4}[\epsilon^{lmn}q_l(1)q_m(2)q_n(4)q_i(3)\bar{q}^i(5) \\
&\quad - \frac{1}{3}\epsilon^{lmn}q_l(1)q_m(2)q_n(3)q_i(4)\bar{q}^i(5)] \\
&= |C_2\rangle, \\
[\{(123)_1 4\}_3 5_{\bar{3}}]_1 &= \frac{1}{3\sqrt{2}}\epsilon^{lmn}q_l(1)q_m(2)q_n(3)q_i(4)\bar{q}^i(5) \\
&= |C_3\rangle. \qquad \text{(B5)}
\end{aligned}$$

Now we prove that the three color singlets in Eq. (17) are the same as Eq. (B5). To begin with, we can represent the $\{(12)_{\bar{3}}3\}_8$ corresponding to a Young-Yamanuchi basis of the Young tableau [21] in Eq. (15) as a traceless rank (1,1) form, as follows:

$$\begin{aligned}
\{(12)_{\bar{3}}3\}_8 &= \epsilon^{ikl}q_k(1)q_l(2)q_j(3) \\
&\quad - \frac{1}{3}\delta^i_j\epsilon^{lmn}q_l(1)q_m(2)q_n(3). \qquad \text{(B6)}
\end{aligned}$$

As for the other $\{(12)_6 3\}_8$ state, corresponding to the other Young-Yamanuchi basis of the Young tableau [21], we use the following formula,

$$\{(12)_6 3\}_8 = \frac{2}{\sqrt{3}}\left[(23)\{(12)_{\bar{3}}3\}_8 - \frac{1}{2}\{(12)_{\bar{3}}3\}_8\right], \qquad \text{(B7)}$$

where (23) is the permutation operator. Furthermore, using the following useful formula,

$$\begin{aligned}
&\delta^i_j\epsilon^{lmn}q_l(1)q_m(2)q_n(3) \\
&\quad = \epsilon^{ikl}q_k(2)q_l(3)q_j(1) - \epsilon^{ikl}q_k(1)q_l(3)q_j(2) \\
&\qquad + \epsilon^{ikl}q_k(1)q_l(2)q_j(3), \qquad \text{(B8)}
\end{aligned}$$

we can represent $\{(12)_6 3\}_8$ as follows:

$$\begin{aligned}
\{(12)_6 3\}_8 &= \frac{1}{\sqrt{3}}[\epsilon^{ikl}q_k(2)q_l(3)q_j(1) \\
&\quad + \epsilon^{ikl}q_k(1)q_l(3)q_j(2)]. \qquad \text{(B9)}
\end{aligned}$$

It is easily seen that $\{(12)_6 3\}_8$ is symmetric under the exchange of particles 1 and 2. The remaining part of the Young-Yamanuchi basis of the Young tableau [21] in Eq. (16) can be represented as the traceless rank (1,1) tensor

$$(45)_8 = q_i(4)\bar{q}^j(5) - \frac{1}{3}\delta^j_i q_l(4)\bar{q}^l(5). \qquad \text{(B10)}$$

We can now show that $[\{(12)_6(34)_{\bar{3}}\}_3 5_{\bar{3}}]_1$ and $[\{(12)_{\bar{3}}34\}_3 5_{\bar{3}}]_1$ in Eq. (B5) are obtained by combining $\{(12)_6 3\}_8$ and $\{(12)_{\bar{3}}3\}_8$ with Eq. (B10), respectively, through contraction and normalization.

In addition, it is easy to see that the Young-Yamanouchi bases of the Young tableau [211] in Eq. (13) can be obtained from combining $(123)_1$, $\{(12)_6 3\}_8$, and $\{(12)_{\bar{3}}3\}_8$ with $q_i(4)$ through contraction and normalization, resulting in a rank (1,0) tensor.

APPENDIX C: INDEPENDENT COLOR BASIS

The three color singlet states in Eq. (B5) form a complete set of color basis for the color singlet pentaquark. We can construct another complete set of color bases for the color singlet pentaquark, by exchanging any two particles among particles 1–4. A complete set of color basis obtained by exchanging particles 3 and 4 is given by

$$\begin{aligned}
|C'_1\rangle &= \frac{1}{4\sqrt{3}}[\epsilon^{lmn}q_l(1)q_m(4)q_n(3)q_i(2)\bar{q}^i(5) \\
&\quad + \epsilon^{lmn}q_l(2)q_m(4)q_n(3)q_i(1)\bar{q}^i(5)], \\
|C'_2\rangle &= \frac{1}{4}[\epsilon^{lmn}q_l(1)q_m(2)q_n(3)q_i(4)\bar{q}^i(5) \\
&\quad - \frac{1}{3}\epsilon^{lmn}q_l(1)q_m(2)q_n(4)q_i(3)\bar{q}^i(5)], \\
|C'_3\rangle &= \frac{1}{3\sqrt{2}}\epsilon^{lmn}q_l(1)q_m(2)q_n(4)q_i(3)\bar{q}^i(5). \qquad \text{(C1)}
\end{aligned}$$

Furthermore, the complete set in Eq. (C1) is related to that in Eq. (B5) through an orthogonal transformation as follows:

$$\begin{aligned}
|C'_1\rangle &= -|C_1\rangle, \\
|C'_2\rangle &= -\frac{1}{3}|C_2\rangle + \frac{2\sqrt{2}}{3}|C_3\rangle, \\
|C'_3\rangle &= \frac{2\sqrt{2}}{3}|C_2\rangle + \frac{1}{3}|C_3\rangle. \qquad \text{(C2)}
\end{aligned}$$

It should be noted that the set in Eq. (C1) takes the form of linear sums of the product of a color singlet baryon and a color singlet meson, but with different quarks forming the baryon and meson states.

When we combine Eq. (B4) with $\bar{q}^i(5)$ through contraction, we can obtain a useful formula that constrains the four color singlet baryon meson states appearing in the right-hand side of Eq. (C1) through the following equation:

$$\frac{1}{3\sqrt{2}}\epsilon^{lmn}q_l(1)q_m(2)q_n(3)q_i(4)\bar{q}^i(5)$$
$$= \frac{1}{3\sqrt{2}}\epsilon^{lmn}q_l(1)q_m(2)q_n(4)q_i(3)\bar{q}^i(5) - \frac{1}{3\sqrt{2}}\epsilon^{lmn}q_l(1)q_m(3)q_n(4)q_i(2)\bar{q}^i(5) + \frac{1}{3\sqrt{2}}\epsilon^{lmn}q_l(2)q_m(3)q_n(4)q_i(1)\bar{q}^i(5). \tag{C3}$$

Therefore, the independent color set can also be expressed in terms of three independent states that are expressed as products of a color singlet baryon and a color singlet meson configuration. One possible choice for the independent set composed of a color singlet baryon and a color singlet meson is given as follows:

$$\frac{1}{3\sqrt{2}}\epsilon^{lmn}q_l(1)q_m(2)q_n(4)q_i(3)\bar{q}^i(5) = \frac{2\sqrt{2}}{3}|C_2\rangle + \frac{1}{3}|C_3\rangle,$$
$$\frac{1}{3\sqrt{2}}\epsilon^{lmn}q_l(1)q_m(3)q_n(4)q_i(2)\bar{q}^i(5) = \sqrt{\frac{2}{3}}|C_1\rangle + \frac{\sqrt{2}}{3}|C_2\rangle - \frac{1}{3}|C_3\rangle,$$
$$\frac{1}{3\sqrt{2}}\epsilon^{lmn}q_l(2)q_m(3)q_n(4)q_i(1)\bar{q}^i(5) = \sqrt{\frac{2}{3}}|C_1\rangle - \frac{\sqrt{2}}{3}|C_2\rangle + \frac{1}{3}|C_3\rangle. \tag{C4}$$

[1] M. Gell-Mann, Phys. Lett. **8**, 214 (1964).
[2] M. Y. Han and Y. Nambu, Phys. Rev. **139**, B1006 (1965).
[3] R. L. Jaffe, Phys. Rev. D **15**, 267 (1977).
[4] R. L. Jaffe, Phys. Rev. D **15**, 281 (1977).
[5] S. K. Choi *et al.* (Belle Collaboration), Phys. Rev. Lett. **91**, 262001 (2003).
[6] N. A. Tornqvist, Z. Phys. C **61**, 525 (1994).
[7] C. E. Thomas and F. E. Close, Phys. Rev. D **78**, 034007 (2008).
[8] I. W. Lee, A. Faessler, T. Gutsche, and V. E. Lyubovitskij, Phys. Rev. D **80**, 094005 (2009).
[9] P. Wang and X. G. Wang, Phys. Rev. Lett. **111**, 042002 (2013).
[10] V. Baru, E. Epelbaum, A. A. Filin, F.-K. Guo, H.-W. Hammer, C. Hanhart, U.-G. Meiner, and A. V. Nefediev, Phys. Rev. D **91**, 034002 (2015).
[11] A. Hosaka, T. Iijima, K. Miyabayashi, Y. Sakai, and S. Yasui, Prog. Theor. Exp. Phys. **2016**, 062C01 (2016).
[12] E. S. Swanson, Phys. Lett. B **588**, 189 (2004).
[13] C. Y. Wong, Phys. Rev. C **69**, 055202 (2004).
[14] L. Maiani, F. Piccinini, A. D. Polosa, and V. Riquer, Phys. Rev. D **71**, 014028 (2005).
[15] D. Ebert, R. N. Faustov, and V. O. Galkin, Phys. Lett. B **634**, 214 (2006).
[16] W. Chen and S. L. Zhu, Phys. Rev. D **83**, 034010 (2011).
[17] H. Hogaasen, J. M. Richard, and P. Sorba, Phys. Rev. D **73**, 054013 (2006).
[18] Y. Cui, X. L. Chen, W. Z. Deng, and S. L. Zhu, HEPNP **31**, 7 (2007).
[19] F. Buccella, H. Hogaasen, J. M. Richard, and P. Sorba, Eur. Phys. J. C **49**, 743 (2007).
[20] M. Padmanath, C. B. Lang, and S. Prelovsek, Phys. Rev. D **92**, 034501 (2015).
[21] R. Aaij *et al.* (LHCb Collaboration), Phys. Rev. Lett. **115**, 072001 (2015).
[22] Z. C. Yang, Z. F. Sun, J. He, X. Liu, and S. L. Zhu, Chin. Phys. C **36**, 6 (2012).
[23] R. Chen, X. Liu, X. Q. Li, and S. L. Zhu, Phys. Rev. Lett. **115**, 132002 (2015).
[24] S. Takeuchi and M. Takizawa, Phys. Lett. B **764**, 254 (2017).
[25] J. He, Phys. Lett. B **753**, 547 (2016).
[26] L. Maiani, A. D. Polosa, and V. Riquer, Phys. Lett. B **749**, 289 (2015).
[27] S. Takeuchi and M. Takizawa, Phys. Lett. B **764**, 254 (2017).
[28] R. K. Bhaduri, L. E. Cohler, and Y. Nogami, Nuovo Cimento A **65**, 376 (1981).
[29] W. Park, A. Park, and S. H. Lee, Phys. Rev. D **92**, 014037 (2015).
[30] J. Q. Chen, J. L. Ping, and F. Wang, *River Edge, USA* (World Scientific, Singapore, 2002), p. 574.
[31] F. Stancu and S. Pepin, Few-Body Syst. **26**, 113 (1999).
[32] W. Park, A. Park, and S. H. Lee, Phys. Rev. D **93**, 074007 (2016).
[33] D. Melikhov and B. Stech, Phys. Rev. D **74**, 034022 (2006).